Automatika

Journal for Control, Measurement, Electronics, Computing and Communications

ISSN: (Print) (Online) Journal homepage: www.tandfonline.com/journals/taut20

A cross layer graphical neural network based convolutional neural network framework for image dehazing

M. Pavethra & M. Uma Devi

To cite this article: M. Pavethra & M. Uma Devi (2024) A cross layer graphical neural network based convolutional neural network framework for image dehazing, Automatika, 65:3, 1139-1153, DOI: 10.1080/00051144.2024.2346964

To link to this article: https://doi.org/10.1080/00051144.2024.2346964

Published online: 09 May 2024.

AUTOMATIKA
2024, VOL. 65, NO. 3, 1139–1153
https://doi.org/10.1080/00051144.2024.2346964

A cross layer graphical neural network based convolutional neural network framework for image dehazing

M. Pavethra and M. Uma Devi

Department of Computing Technologies, SRM Institute of Science and Technology, Kattankulathur, Tamil Nadu, India

ABSTRACT

The current version of imaging equipment cannot quickly and effectively make up for the reduction of visibility triggered by bad weather. Traditional strategies minimize hazy impacts by employing an image depth model and a physical model. Following experts, erroneous depth data reduces the efficacy of the dehazing algorithm. Dehazing methods based on CNN are imperfect to handle region which is bright or similar to atmospheric light and thus leads to oversaturation of pixels. These challenges can be addressed by proposing a novel model that incorporates the idea of a Graphical Neural Network. The amount of light coming from the atmosphere is estimated using normalization where the contrast of the image gets adjusted using Bias Contrast stretch Histogram Equalization. An enhanced Transmission map estimator is used to render the hazy scene. Finally, the cross-layer graphical neural network-based CNN model is applied to produce a haze-free image and eliminate the over-saturation of pixels. Extensive evaluation findings show that the proposed approach can significantly recuperate misty imagery, even if the images have a substantial amount of haze.

ARTICLE HISTORY
Received 28 November 2023
Accepted 19 April 2024

KEYWORDS
Image dehazing; Bias Contrast Stretch Histogram Equalization; enhanced transmission map; cross-layer graphical neural network

1. Introduction

Photos taken with cameras, smartphones, or computers always need to undergo post-processing to improve their aesthetic appeal and usefulness in a variety of application scenarios, such as object recognition and detection. Raising the visual quality, including visibility, contrast, and brightness, is one of their key objectives.

The hazy substrate in the surroundings often degrades exterior photographs. The perception of the scene can be greatly diminished by atmospheric abnormalities. [1]. As the illumination travels from the eye to the lens, these particles consume and diffuse it, leading to blurry images which typically lack perceptual luminance and consequently give imagery depletion [2]. The Mortal Perception System (MPS) implies visuals that are linked to actual notions. Computers are unable to learn human visual abilities. To learn the perceived things, specific algorithms and applications are required. To replace the human visual system, Computer Vision Technology (CVT) made it possible for any visual activity to be processed quickly and simply.

CVT, a discipline of computer science, aims to replicate some of the nuances of a vision-based system so that machines may recognize and grasp images and videos in the same way that humans do. Systems that utilize computer vision strive to mimic human perception. These tools can help computers process and respond to visual input more efficiently.

1.1. Haze formation model

Traditionally, haze is an environmental abnormality that impairs visual perception in computers. Attenuation and airlight are combined to create haze. Images are usually captured in a wide range of atmospheric circumstances. With the line of sight, the intense light that the camera captures fades [3]. The term "airlight" refers to the light coming from all directions. A blend of incident light from the camera and a skylight gives more white pixels to the image. Figure 1 depicts the haze formation process.

Figure 1 illustrates the haze formation process in three main steps. First, sunlight enters the atmosphere; it comes into contact with microscopic particles such as dust and pollution, which scatters the light in different directions. Second, the dispersed light eventually makes its way to the camera, giving the picture an unclear appearance. The amount and size of the particles, as well as how far light travels through the atmosphere, all have an impact on how intense this haze is. In the end, this series of occurrences results in impaired visual perception and difficulties with picture processing, especially in situations with low contrast, low colour saturation, and high brightness. For computer vision applications to build effective dehazing solutions, it is imperative to comprehend this haze creation process. Haze can be characterized as a linear framework, while obscurity is outlined by the Atmospheric Scattering model, which

CONTACT M. Pavethra pavethra93@gmail.com
This article has been corrected with minor changes. These changes do not impact the academic content of the article.

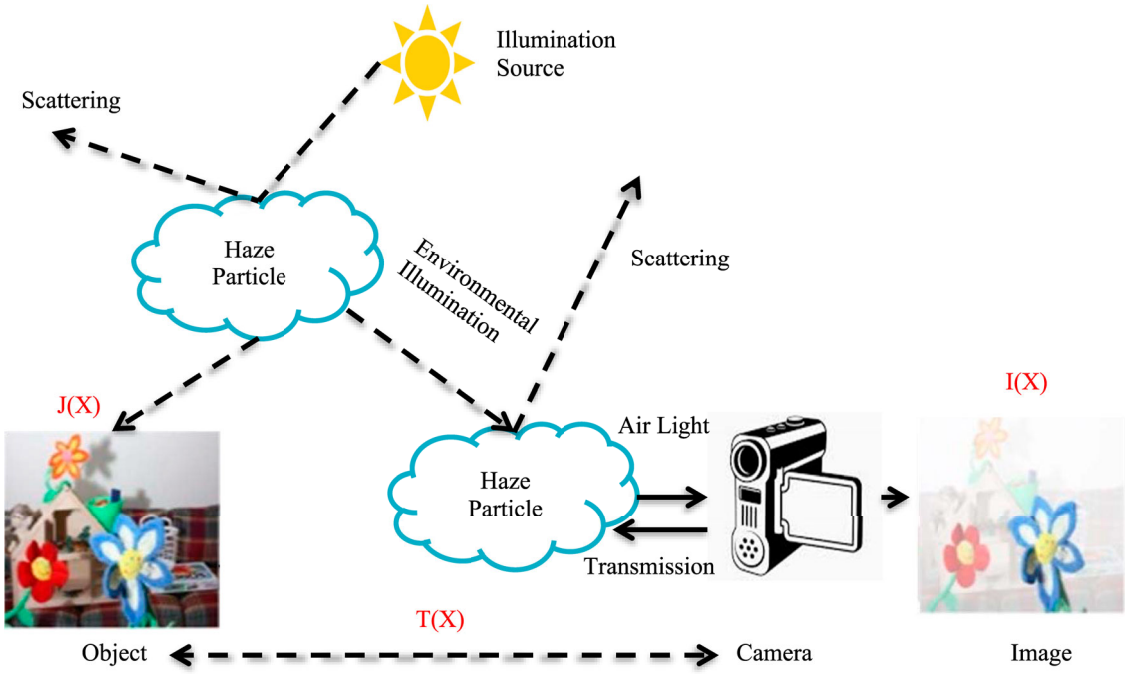

Figure 1. Haze Image Formation.

is illustrated below:

$$s(x) = P(x) * Q(x) + A(1 - Q(x)) \quad (1)$$

The above equation describes, $s(x)$ represents the observed intensity of light at a given pixel location x on the screen. The term $p(x)$ denotes the intrinsic intensity of light emitted by objects in the scene, while $Q(x)$ represents the fraction of light that reaches the camera from these objects. The parameter A corresponds to the natural ambient light of the atmosphere, which contributes to the overall observed intensity $s(x)$ when light is scattered or obscured along its path. Poor contrast, low colour saturation, and strong brightness are issues with natural images taken during hazy conditions. Processing sophisticated vision tasks using haze images as input can become substantially more challenging.

Dehazing refers to haze elimination strategies that attempt to elevate the perceived quality of visuals degraded by mist particles that reflect light. Dehazing the image is a crucial step before carrying out advanced vision activities [4]. By boosting the contrast and highlighting the fine details, conventional techniques increase the visual impact of foggy images. Image Intensification Strategies and Picture Preservation Methods (PPM) [5] may both conduct single-image dehazing. Formerly, visual augmentation [6] innovations failed to establish the main cause of image degradation and instead focused on improving image-distinctive features. Probabilistic Equalization, Wavelet assessment, and Retinex hypothesis, for example, aimed towards enhancing visual contrast without using any physical models.

PPM builds a framework by recognizing the physical principles of ocular pictures, extrapolating the degrading process, and mitigating the aberrations triggered by these pictures. Using Prior-Based (PB) approaches combined with air scattering theory, the preciseness of the depth map may be accurately estimated. Several PB methods were presented to separate ambient light from the source image.

Based on the Haze-Lines method [7], the hues of an image without haze could be represented by hundreds of various colours. Color Attenuation Prior [8] employs a linear model of a pixel's hue and intensity to estimate the spatial extent of a scene. Assessing the transmission will restore the radiance. It was possible to discriminate between sky and dark areas using near-thermal radiation [9]. Picture matting was developed to calculate feature map deviation. The Atmospheric veil correction approach resulted in the production of a transmit sequence for typical sectors and a transmit map. These techniques, however, did not distinguish between the structure and texture of fuzzy images. In general, Prior-based approaches use ASM to accomplish dehazing, which causes inaccurate estimation of the transmission map because the prior may be easily broken.

Another method for addressing the dehazing issue is image fusion technology. When using these techniques, blurry images are often enhanced using specific enhancement technologies. Then, using a particular fusion approach, the images are combined, and the resulting image is referred to as being dehazed [10]. Applying white rebalancing converts the blurry picture into the photograph, and subtracting the mean brightness value of the entire hazy image from the first hazy image transforms the second hazy image into the other image. The brightness, chromaticity, and saliency of the

original images are then taken into account during the fusion of both these images. After applying Normalized Gamma correction to the shaky photos, they are integrated utilizing multi-scale picture fusion technology. The four photos with their intensities modified are then blended to create the final, haze-free image.

Deep Learning (DL) and artificial intelligence (AI) have advanced to the point that they can learn useful representations of features directly from data. Since DL models recognize complex patterns Learning-based Based Dehazing methods were proposed. [11] finds low-intensity pixels by applying a filter. [12] Structural and statistical attributes of hazy images are captured. [15–18] Relevant features are extracted through a designed network that generates a transmission map. Encoder decoder architecture is adopted in DL-based methods. Skip connections are added from convolution layers to yield better dehazed results.

The results of dehazing are strongly impacted by photos having colour artefacts. This has led to a noticeable rise in normalization-based image dehazing techniques. Even though learning-based techniques must evaluate the atmospheric light and transmission map, they do not concentrate on non-spatial pixel aspects. Because of this, learning-based techniques fail (1) to influence the area that is bright or similar to atmospheric light, which causes an issue with supersaturation and (2) inaccurate transmission map estimates. This gave rise to the proposed approach that emphasizes Cross Layer Graphical Neural Network as a means of eradicating the monochromatic super saturation issue.

The novelty of the proposed approach lies in integrating a Graphical Neural Network with Bias Contrast Stretch Histogram Equalization and Enhanced Transmission Map Estimation to effectively address even and uneven haze in indoor images, overcoming limitations of existing dehazing methods based on CNN and mitigating issues such as oversaturation in bright regions. The cross-layer graphical neural network-based CNN model uniquely enhances visibility in misty scenes, offering a robust solution for haze reduction in diverse atmospheric conditions.

Contributions of this article

- The model emphasizes on the aspect change area throughout the rebuilding process, and the model's ability to discriminate between fuzzy pictures is strengthened by dehazing the feature difference information at various stages rather than all at once.
- Graphical neural network models are presented with a full examination. Additionally, research on theoretical and empirical investigations of GNN models is discussed.
- Vision spatial distortions, such as perceived loss and pixel-centric Eculidean loss, can be reduced by utilizing an improved transmission map. As a result, solutions that are more aesthetically pleasant can be offered.

The remaining portion of the article is divided into the following parts. Section II presents the literature review for this subject. Section III provides a detailed explanation of the proposed method for the transmission map estimation-based image dehazing algorithm. Section IV concludes with the results and discussion. Section V provides an overview of the article.

2. Literature review

Despite the simplicity of conventional image dehazing techniques, their effectiveness is constrained by the challenge of locating global prior information. In recent times, methods that utilize CNN have seen widespread use in the computer intelligence sector. Dehazing strategies based on deep learning can be broadly classified into two types. The first group creates transmission maps using network learning. It then calculates the atmospheric light estimation and determines the outcomes of the image dehazing. The second category, which does not rely on ASM, uses network learning to produce picture-dehazing results directly.

A duplex-stream visual hazing dazzling network called HDNet was developed by [10]. It can distinguish between images that are artificially and naturally hazy. The first stream retrieves properties especially from the picture saturation channel, while the second stream gathers information on hazy distribution from the dark channel and grey level co-occurrence matrix. For real-time computer vision applications, Som and Jatoth [11] developed a quick and effective image dehazing solution with decreased computing complexity. Dehazing image is a crucial problem that has been widely studied in image processing and computer vision. The technique was first created and tested for single photos before being expanded to real-time images. This DCP approach produced erroneous transmission and distorted output since it failed at a few unique sequences. Because of the dispersion of the haze particles in the environment, Figure 2 depicts the model of how a haze forms in an image.

Singh et al. [12] concentrated on describing a few key methods, particularly GANs, to address the issue of dehazing. The advantages and disadvantages of the various methods have been presented after being qualitatively assessed. The relevance of dehazing and its applicability in the actual world are finally discussed. Dehazing images are one of the most difficult computer vision jobs. For adaptive residual learning, Preethi et al. [13] employed an attenuation module to filter away features from the preceding layers that are unnecessary. Notably, meticulous residual learning and wavelength-driven multi-categorical design are not advised for UIR. To allow underwater vision, pre-processing techniques

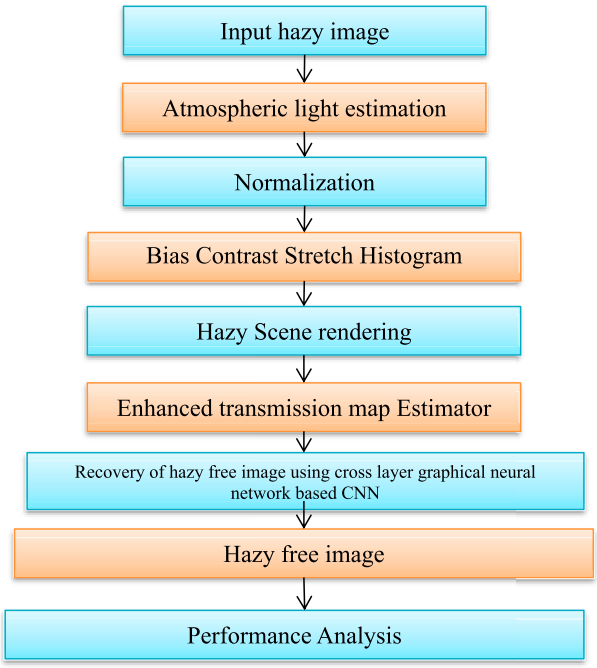

Figure 2. Progression of the suggested methodology.

for low-quality image augmentation are needed since underwater lighting is limited.

End-to-end tightly coupled coder decoder-based GAN was used by Parihar et al. [14] to dehaze a picture from a foggy input image, making it easier to extract and use image features. To optimize and enhance the use of the obtained traits, a Contrast-aware Channel Attention Module was developed. As a result, we were able to create dehazed photos that were more appealing and realistic-looking, with better edges and structure recognition. The "Multiple-Factor Fusion Cascade Network (MFFCN)", which combines a multi-patch image codec, a multi-channel feature enhancement module, and a multi-level feature fusion module, formed the foundation for the IR image dehazing technique created by Gao [15].

The multi-patch image encoder, which blends characteristics from numerous picture patches to increase responsiveness for varying quantities of haze in various regions, is immediately removed using this technique. A multi-channel feature enhancement module that might promote interactions among various attributes and expand the spectrum of discovered illustrations. The capacity to find and recognize items at a distance will be significantly impacted by this. Using CNN and a multi-scale deep residual learning network developed by Joy and Jayasree [16], a hazy picture is mapped to its matching haze-free image to produce a dehazed output image. A multiscale residual network's core element passes through the output of one layer while feeding it to the next. Ayoub et al. [17] modified the optimal dehazing technique by pre-processing frames to reduce noise and restricted dynamic range before dehazing. As a result of sensor measurement mistakes, all frames include some noise and a restricted dynamic range, which may be disregarded and enhanced throughout the haze removal process.

There are several issues with the image in public spaces, including the hazing issue. Yoon and Cho [18] developed an image-dehazing network to enhance detection performance in bad weather owing to haze and limited visibility. The network analyzes the meteorological conditions at the moment and uses the haze level to remove haze.

The two YOLO object detectors get the recovered image along with the thermal image, which allows them to more accurately identify moving objects. Late fusion is used to improve object recognition performance. The channel mechanism of attention constitutes a base for the broad image-dehazing neural network paradigm created by Guo et al. [19].

A network structure made up of modules for multi-scale residual, channel attention, and encoding-decoding is the main component of this approach. They undertake qualitative as well as quantitative research on artificial and actual databases to show the resilience of the proposed dehazing network model. Alenezie et al [20] created a technique for calculating scene depth using pixel differences between patches both local and global. The channels that comprise the pixel variance are red and blue, green and red, and green and blue. These channels are not included in the absolute mean luminosity estimates. Underwater image enhancement has not received enough attention, which leaves the potential for more study.

A network with three deep CNNs that can dehaze 4 K images in real-time on a single GPU was created by Zheng et al [21]. The first CNN extracts haze-relevant characteristics from the hazy input at a reduced resolution before fitting locally affine models in the bilateral space. The majority of current deep dehazing methods are computationally demanding, which prevents their use for high-resolution photos, particularly for UHD or 4 K resolution images. Two strategies for the hardware implementation of the picture de-hazing algorithm are provided by [22]. This work proposes the grey image-based, pixel-wise dehazing method. The ability to predict an accurate transmission map is the main benefit of the suggested strategy.

Fog drastically reduces the quality of the image that is collected, which not only jeopardizes the surveillance system's dependability but also creates a risk. Two objectives are set forth by Likhitaa and Anand [23] and are carried out. The initial goal is to contrast deep learning and machine learning models for hazy and clear image categorization. The second goal is to use a potent deep neural network to analyze foggy images to remove them. The key challenge at hand is creating a system that can both detect the presence of haziness and provide a workable solution to get rid of it. Ismail et al. [24] proposed a properly organized, adaptable

end-to-end CNN utilizing a semi-supervised framework that restores perception in a variable environment. The training set for the suggested deep learning network includes both synthetic and real-world fuzzy pictures, and it is composed of decoupling CNNs. Zhai et al. [25] address the rising prevalence of autism in children and propose an interactive educational framework utilizing Machine Learning-based Virtual Reality Applications to enhance learning experiences for mentally challenged children, incorporating physical exercise and cognitive methods for improved lifestyle and skill development.

Bi et al. [26] introduces a rapid single-image dehazing algorithm that utilizes a piecewise transformation model between the minimum channels of hazy and haze-free images. By incorporating quadratic and linear functions for dark and bright regions, respectively, along with an adjusted haze optical model, the proposed algorithm demonstrates superior performance with minimal artifacts and colour distortion. Li et al. [27] addresses the challenge of single image dehazing in highway tunnels by proposing a novel algorithm based on artificial multi-exposure image fusion. The method leverages gamma correction, guided filter-based two-scale decomposition, and linear saturation adjustment to efficiently enhance visibility, yielding clear and vibrant haze-free images in a fast and effective manner.

Zheng et al. [28] introduces a novel single-image dehazing approach, PADMEF, which integrates adaptive structure decomposition and multi-exposure image fusion. Unlike existing methods, PADMEF focuses on local enhancement, effectively removing haze-induced visual degradation without relying on physical model inversion, depth estimation, or costly refinement processes. Zhu et al. [29] introduces a novel dehazing algorithm specifically tailored for remote sensing images, addressing challenges posed by suspended aerosols under varying weather conditions. The proposed method employs a differentiable function for scene depth modelling, atmospheric light estimation, and transmission map calculation.

In order to reduce aberrations in the brightest regions of the image and enhance overall image clarity, weakening techniques are applied in the study [30]. In order to precisely estimate atmospheric light, a quadtree subdivision-based additional channel approach is utilized, with average greys and gradients serving as evaluation criteria. Ultimately, the atmospheric scattering model is used to create a haze-free image, showing that the algorithm's linear time complexity allows for rapid processing and good image recovery, particularly at depth edges. The paper [31] presents a novel image Dehazing method that adheres to the fundamental assumptions of a physical haze model instead of inverting it. By underexposing the fuzzy image using gamma correction, depth estimation and refinement procedures are avoided. Then, to combine these underexposed photos into a haze-free output, a multi-scale Laplacian blending technique is applied.

2.1. Problem statement

The atmospheric light is a major challenge to processing hazing images because it scatters light and attenuates light. As a result of all these factors, hazing images suffer greatly and their visibility and contrast are affected. This paper discusses image enhancement techniques and image quality enhancement using filters. Bias Contrast Stretch Histogram Equalization (BCSHE) has been proposed as a method for removing hazy images that suffer from "significant contrast, texture, edge, and color deterioration". It is used to estimate the transmission of input images from ambient light. With this method, the haze can be removed and the image which has less amount of hazing and a more improved image can be achieved, but the actual colour contrast and equalization are not improved.

3. Research methodology

The framework for image dehazing based on a cross-layer graphical neural network and a convolutional neural network will be thoroughly discussed in the following section. Figure 2 depicts the way the proposed approach has evolved. The normalizing method can be used to calculate the amount of light coming from the atmosphere. After an image has been standardized, BCSHE is employed to modify the intensity so that it accurately reflects the atmospheric conditions in the image. The rendering process employs the enhanced transmission map estimator to produce the foggy scene. The CLGNN-CNN model is then utilized to produce the picture without haze. This is done to lessen the issue of pixels becoming over-saturated which is related to the various haze reduction techniques now in use.

By strategically integrating Graph Convolutional Layers, Graph Pooling Layers, and Fully Connected Layers and utilizing non-linear activation functions, the suggested CLGNN-CNN structure is found to be effective. This architecture addresses the particular difficulties related to image dehazing by providing a logical and flexible framework for thorough feature extraction, cross-layer fusion, and effective classification. By combining multiple feature representations and refining the dehazing process with adaptive architecture, the CLGNN-CNN model successfully improves visibility in foggy environments.

3.1. Dataset collection

A transport dataset accessible on the Kaggle open data website is employed to evaluate the efficacy of the suggested architectural layout. Figure 3 displays a subset of

Figure 3. Sample dataset.

Algorithm 1 Process of ALE

Input: $l(p, q, r) \in \mathbb{K}^{P\times Q\times R}$: Hazy Source Image
$s^{dark}(p, q) \in \mathbb{K}^{P\times Q}$**:** Dark Channel of Hazy Image.
Output:$E \in \mathbb{K}^{1\times P}$**:** ALE
andp1 $[val, ind] = \max_{j=0}^{q}(s^{dark}(p, q)\ s(p, q))$
//Determine the q number of bright pixels and the positions of those pixels using the s^{dark} image
Step 2 for $i \leftarrow 1$ ***to C do***
Step 3 $s(1, j) = l(ind, j)$
// determine the q pixels of each channel that are situated at the places *ind*.
Step 4 End
Step 5 $E = \frac{s(1,X)}{q}$;
// Estimate the mean of $s(1, X)$

the dataset that was used for the study. The image has 2160 and 3840 pixels in height and width, respectively.

3.2. Atmospheric Light Estimation (ALE)

Scattering and attenuation are both caused by the reflection of particles in the atmosphere that are suspended, such as fog, haze, and mist. The light that is transmitted directly from the location to the lens is reduced due to dispersing and diminution, developing a supplementary layer of ambient light that is made up of the encompassing dispersed light. Equation (2) describes the mathematical model for the development of fuzzy images.

$$l(p, q, r) = s(p, q, r)u(p, q) + E(1 - u(p, q))p, q \in \mathbb{K}^{P\times Q} \quad (2)$$

where E is the ambient light value, $s(p, q, r)$ is the scene radiance, and $u(p, q)$ is the scene transmission medium - defining the amount of light that is not dispersed and reaches the camera. $l(p, q, r)$ is the acquired hazy image. Finally, the number of channels is represented by p, $\in \mathbb{K}^3$, and the coordinates of the pixels are denoted by $(p, q) \in \mathbb{K}^{P\times Q}$. The quality of the input images is diminished due to the atmospheric light; hence, an appropriate approach is necessary to estimate the atmospheric light There are a few different approaches to use when calculating the amount of light coming from the atmosphere. Estimates of the atmospheric light in each colour channel have been produced for this investigation using the procedures outlined in Algorithm 1. This would have the effect of transforming the surrounding light into a three-dimensional vector $E \in \mathbb{K}^{1\times P}$, where each value represents the atmospheric light for a single channel.

3.3. Normalization

Most data mining systems use some kind of normalization as a preprocessing step. A dataset's attribute values are normalized such that they all lie inside a predetermined interval, often between 0.0 and 1.0. Normalization is a pre-modelling step that smoothes and normalizes the data. The technique is easier to put into practice if standard mathematical transformations are used [32]. Here, we choose the z-score normalization method, although other common approaches include "min–max normalizing", "z-score normalization", and "decimal scaling method".

- **Z-score normalization**

Every input feature vector is adjusted by employing the Z-score normalization strategy. Applying the above approach, the average and Standard Deviation (SD) of each feature within a training data set are obtained and then divided by the entire amount of attributes in the training data collection. This technique is also known as zero-mean normalization. For every single attribute, the mean and standard deviation are calculated. It is necessary to perform the subsequent transformation, as indicated by the general formula:

$$a' = \frac{(y - \mu)}{\sigma} \quad (3)$$

Where the average is μ and the SD sigma for the value of the attribute a that is being considered: Before beginning the training process, the z-score normalization technique is performed on every feature that is included in the data set. After the standard deviation and mean for each feature have been computed based on a set of training data, it is essential to maintain these values to utilize them as weights in the design of the system [33].

3.4. Bias Contrast Stretch Histogram Equalization (BCSHE)

BCSHE is a technique that is used to increase the contrast in images, and it is commonly used and extremely efficient. The greyscale levels of the input image are remapped with the use of a "cumulative density function (CDF)".

Assuming that $F_x \in \{0, y-1\}$, let F_x be the average of the image i. By F_x, the picture is divided into two sub-images, F_x and F_t.

$$i = i_f \cup i_t \tag{4}$$

Where

$$i_f = \{i(x,y) | i(m,l) \leq F_x, \forall i(x,y) \epsilon i\} \tag{5}$$

And

$$i_t = \{i(x,y) | i(x,y) \leq F_x, \forall i(x,y) \epsilon i\} \tag{6}$$

It should be noted that the sub-image i f is composed of $\{F_0, F_1, \ldots, F_x\}$, while the sub-image it is mainly composed of $\{F_{x+1}, F_{x+2}, \ldots, F_{Y+1}\}$

Next, specify the probability density functions for sub-images i_f and i_t as follows:

$$k_f(F_p) = \frac{n_f^p}{n_f} \tag{7}$$

and

$$k_t(F_p) = \frac{n_t^p}{n_t} \tag{8}$$

Where n_f^p and n_t^p are the corresponding values of F_p in the two sub-images i_f and i_t and n_f and n_t are the total values of and $i_f and i_t$ respectively.

subscribee, $n_f = \sum_{p=F_0}^{F_p} n_f^p, n_t = \sum_{p=F_{x+1}}^{F_{Y-1}} n_t^p$ and $n + n_f + n_t$.The corresponding CDFs are then defined as follows:

$$K_t(F_p) = \sum_{p=0}^{F_{t=x}} k_t(F_p) \tag{9}$$

$$K_t(F_p) = \sum_{p=F_{x+1}}^{F_{Y-1}} k_t(F_p) \tag{10}$$

Note 1 byhat $K_t(F_p) = 1$ and $K_t(F_p) = 1$ by definition

Similarly, let's define the following transformations using CDFs

$$J_f(F_p) = F_0 + (F_x - F_0).K_t(F_p) \tag{11}$$

$$J_t(F_p) = F_{x+1} + (F_{x=Y-1} - F_{x+!}).K_t(F_p).K_t(F_p) \tag{12}$$

The histogram's final image may therefore be described as follows:

$$u(x,y) = J(I(x,y)), \tag{13}$$

in which

$$F(F) = \begin{cases} F_0 + (F_x - F_0) \cdot J_t(F_p), & if\ F_p \leq F_x \\ F_{x+1} + (F_{x-1} - F_{x+1}) \cdot J_t(F_p), & \text{else} \end{cases} \tag{14}$$

The output image for the BCSHE approach is depicted in Figure 4.

Figure 4. Output of the BCSHE approach.

3.5. Enhanced Transmission Map Estimator (ETME)

The enhanced transmission map estimator is used to render the hazy scenes. This technique demonstrates the quantity of light that enters the camera after it has been reflected off the subject. The amount of light that the camera records after it has been reflected off the subject is demonstrated through this approach. It is very difficult to de-haze an image if such information about the depth is not available; hence the estimate of the transmission map plays a significant part in the process of image dehazing. Following the steps provided in Algorithm 2, the percentage of light that reaches the camera without being scattered is estimated. On a typical day with no clouds in the sky, there are still some very minute particles in the air; as a result, a fixed component $\omega = [0, 1]$ is presented in Step 5 of Algorithm 2 to maintain the appropriate level of haze for the circumstances of the scenario. Finally, four kinds of output are obtained using an enhanced transmission map estimator which is shown in Figure 5.

Algorithm 2: Enhanced Transmission Map Estimation

Input: I(c, v, x) $\in \mathbb{K}^{C \times V \times X}$: Hazy Source Image, and $E \in \mathbb{K}^{1 \times X}$: Atmospheric Light.
Output: d(c, v) $\in \mathbb{K}^{C \times V}$**:** ETME
Step 1 **for** $i \leftarrow 1$ ***to C do***
Step 2 $\mathrm{I(c, v, j)} = \frac{I(x,V,j)}{E(1,j)}$
// dividing all the pixels of the original image with the corresponding airlight estimation ∗/
Step 3 **End**
Step 4 Compute dark channel
Step 5 $(x,y) \leftarrow 1 - \omega * f^{dark}(x,y)$; // estimation map is computed

3.6. Recovery of hazy free images using cross-layer graphical neural network-based CNN model

This first introduces the proposed CLGNN-CNN. Figure 6 depicts the procedure of the CL graph convolutional neural network. The CLGNN-CNN is composed mostly of three layers: the "Graph Convolutional Layer (GCL), the Graph Pooling Layer (GPL), and the Fully

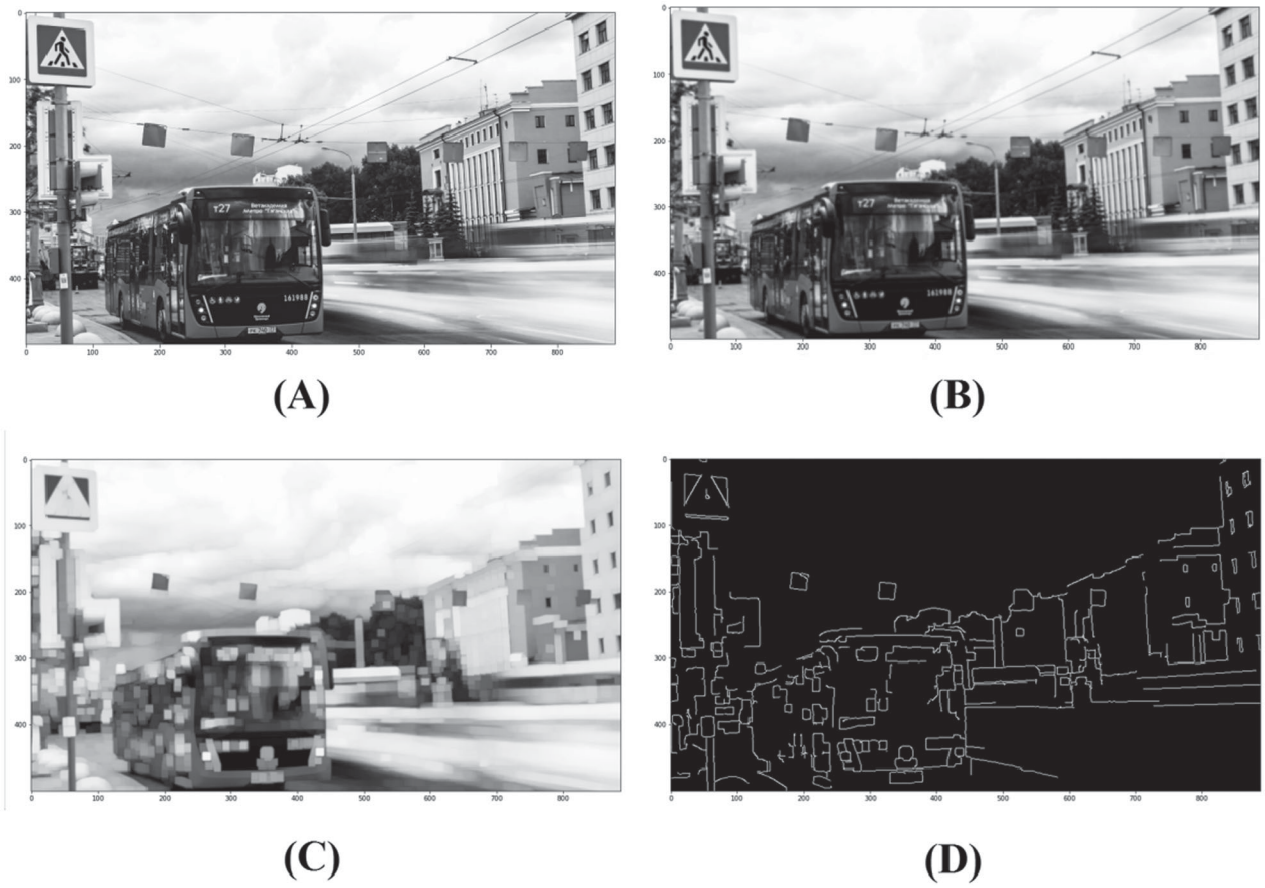

Figure 5. Estimation of transmission map (a) Grey scale image (b) Blurred image (c) Dilatted image (d) Edged image.

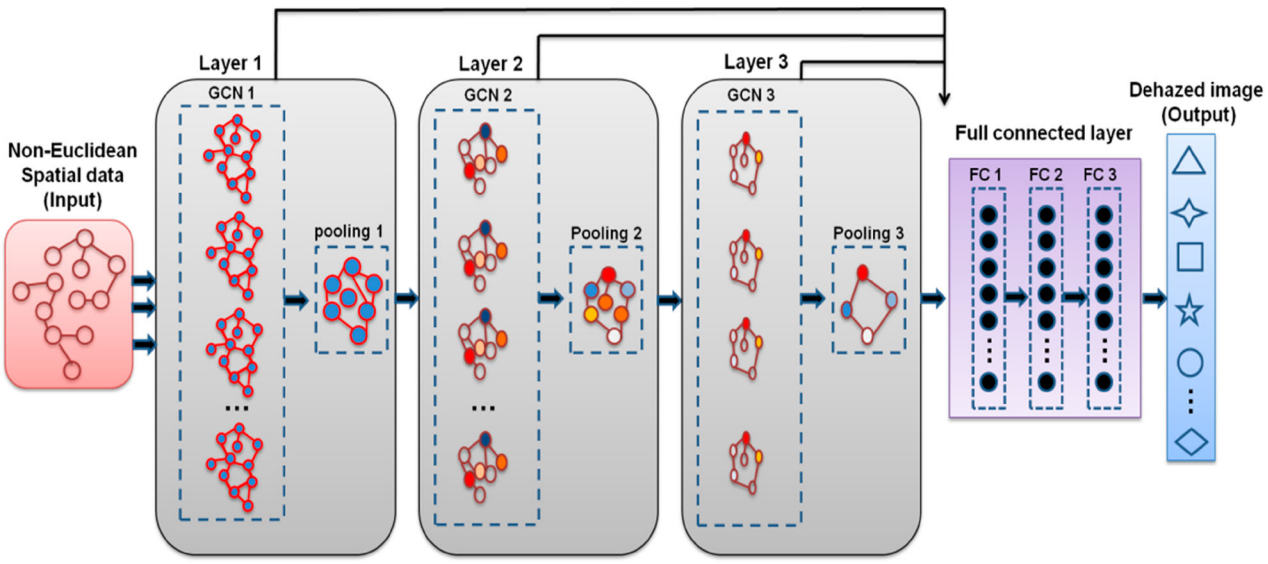

Figure 6. Procedure of cross-layer graph convolutional neural network.

Connected Layer (FL)". Through a Graph Convolution Technique (GCT), the characteristics of the layer and its adjacent layer are collected in the GCL. Effective features are extracted from the image data by the GCL, and the best values of various features are chosen as representatives to represent new layer features by the GPL, which then conducts the GP procedure. High-quality parameters are provided by further GCL or FL classification, substantially reducing the feature dimension at the GCL output. More effective features are obtained in the FCL via several graph convolution and GPL processes. Three FCLs are employed to do graph classification, as opposed to the one layer used by the traditional GCNN.

3.6.1. CLGNN-CNN architecture

In the CLGNN-CNN framework, the local undirected graph structure data that belongs to the kth image in

deep learning is $S_r(V, E, A)i \in k$, assuming that there aisk image generally. The matrix $y_j \in V$ symbolizes the set of layers in the graph framework $a_j, i = (y_j, y_i) \in E$ governs the set of boundaries between layers $c_j \in X$, and A is a symmetric matrix with only 0 or 1 elements. This matrix indicates the interconnection relationship between layers and is a representation of the graph's adjacency matrix. Equation (14) is utilized to amalgamate neighbour layer data and derive highly generalized effective layer characteristics.

$$Z^{f+1} = \sigma\left(\tilde{T}^{-\frac{1}{2}}\tilde{E}\tilde{T}^{-\frac{1}{2}}Z^f U^f\right) \tag{15}$$

where $\tilde{E} = E + J$ indicates adding the identity matrix to the initial proximity matrix to store the layer information. The trainable weight parameter for layer f is indicated by U_f. The initial input data characteristics are represented by Z^0, and the degree matrix is represented $\widetilde{byT}$, where $\tilde{T}_{(j,j)} = \sum_i \tilde{E}_{(j,i)}$.

3.6.2. GPL

In GPL, from the GCL a huge number of useful characteristics are retrieved. The properties collected nevertheless, may be replicated or comparable in nearby layers. Costs associated with computing rise as a result of information redundancy. In common convolutional neural networks, a pooling procedure similar to what is used in neural networks with great generality is needed to acquire the layer characteristics. Consequently, we increase the proposed GPL. Using an adaptive selection process, the graph pooling layer creates a new, smaller graph by convolutioning the layer characteristics.

First, using a trainable variable P, all layer characteristics are projected into One-Dimensional (1D) data. Additionally, the resulting one-dimensional data is used to guide the Top K pooling procedure, which chooses the layer with the greatest score. The pooling process is illustrated in Equation (15).

$$\begin{cases} v_j = \dfrac{c_j^f p^f}{p^f} \\ j_m = top_m(v_j, m) \\ c_j^{f*} = (c_j^f \odot \tanh(v_j))_{j_m} \\ E^* = E_{j_m, j\_m} \end{cases} \tag{16}$$

where $\| \cdot \|$ stands for the two norms, y_i is the 1D vector output of $x_j^f li$ after the learning parameter ρ is applied, $top_m(\cdot)$ chooses the key j_m of the peak mark from the specified input vector, and stands for the $\odot$ multiplication of the vector's corresponding component by component, allocating the appropriate weight $tantoh(v_j)$ to c_j^f. Similarly, a basic multi-layer perceptron is used for training in this research. Backpropagation can be used to learn the tanh function's observable attribute p. Due to its discontinuous output without tanh, the projection vector p cannot be learned by back dissemination.

3.6.3. FCL

In FCL, efficient and reliable summary characteristics were acquired after the preceding three sets of GCN and GP procedures. The feature matrix is inconvenient for tasks requiring categorization or forecasting of these features, hence a classifier is needed to produce the final output. The network topology in this study is thus concluded with three fully linked layers. The retrieved features need to go through some preprocessing, such as cross-layer fusion and dimensional adjustments, before being fed into the fully linked layer. (i) Cross-layer feature aggregation is required since the graph pooling procedure will result in a reduction in the number of layers, which will certainly result in the loss of some relevant information. This procedure may excerpt the features of various scales for processing (different GCL and GPL). Additionally, the information may be efficiently kept for graphs with a limited number of layers. Otherwise, the layers of these short networks may be swiftly eliminated (ii) To enter large-scale feature data into the fully linked layer, those the features. In this process, the concluded graph layer characteristics (i.e. the number of neurons in the FCL) are stored at a specified size. The specifics are displayed in Equation (16)

$$\begin{aligned} y^f &= \left(\frac{1}{M^f}\sum_{j=1}^{M^f} h_j^f\right) ||(MAX(h_j^f)_{j=1}^{M^f}) \\ Y_{lx} &= \sum_{f=1}^{F} y^f \end{aligned} \tag{17}$$

Conventional CNNs feed convolutional data into the fully linked layer after performing a single average or pooling operation. The solution of the proposed method employs to combination of two pooling results. In other words, || stands for the concatenation operation. Following the GCT and GP procedures of each layer, respectively, the layer is first subjected to average pooling and maximum pooling introduces theffeaturesature h_j^f. The two outputs are then combined. Following these procedures, the findings from every layer are added to produce the multi-layer fusion effect.

In Equation (15), M^f signifies the qnumberoflayers, MAX(.) denotes the maximum pooling operation, and Y_{lx} is the feature finally input to the FCL.

3.7. Training of CLGNN-CNN

An NLFA (Step 1), a loss function (Step 2), and an optimizer (Step 3)" compensate the Graphic" Convolutional Neural (GCN) network training. An extensive introduction is provided as follows.

Step 1: The layer features and associated weight matrix serve as the linear input processes for every layer of the CLGNN-CNN. The challenge of classifying graph structures using the CLGNN-CNN is

addressed in this paper. Non-linear classification methods are included in this classification. The effectiveness of the CLGNN-CNN in this research is therefore critically dependent on the Non-Linear Activation Function (NLAF). The sigmoid function and ReLU activation function are used in various network components in this paper. The GCL, the GPL, and the first two FCL are all impacted by the ReLU activation function.

$$sigmoid(c) = \frac{1}{1 + a^{-c}} \tag{18}$$

$$ReLU(c) = \max(0, c) \tag{19}$$

Equation (16) shows that the sigmoid output range is 0 to 1. It's symmetrical and derivable. Classification results are smoother. The partial inverse of the sigmoid function vanishes at very large and very small input values, so it is only used in the last fully connected layer to produce classification results. ReLU is used in the intermediary portion of a CLGNN-CNN to avert gradient disintegration.

Step 2: The training of models is assessed using the loss function. The difference between the label and the estimated value can be quantified with a good loss function. Considering that the kth client's data consists of feature x and label y, $T_r(x, y)$; the labels are coded using one-hot representation; only one digit is used for effective representation; and the labels contain C categories, $v = \ v = [v_1, v_2, \ldots v_x]$. In this study, the layer feature X is input to obtain G as an output G(X), and the GCN model is denoted as G. Equation (18) represents the cross-entropy loss function for the study.

$$f_r(v_j^r, S(c_j^r)) = -\sum_{i=1}^{m_r} [v_j^r log S(c_j^r) + (1 + v_j^r)\log(1 - S(c_j^r)] \tag{20}$$

where m_r is the quantity of data that the r_{th} image and f_r is the associated loss function.

Step 3: The loss function was developed in the previous section and is used to continuously evaluate the benefits and limitations of the current model during the training phase. Stated otherwise, the model is often better if the loss function is lower. Nevertheless, even with an outstanding loss function, it remains ineffective without a means to ascertain the optimal model parameter solution [34]. Model parameters are adjusted by the optimizer to minimize the loss function. "Stochastic gradient descent (SGD)" is the most popular optimizer for neural networks or other machine learning techniques, as shown in Equation (20).

$$\tilde{\theta} = \theta - \eta.\nabla f_r(v^r, S(\theta, c^r)) \tag{21}$$

If the parameter to be optimized is represented by θ, the updated θ parameter is signified by $\tilde{\theta}$, the loss function is denoted by $ł_r(\cdot)$, the gradient is symbolized by ∇, and the step size is represented by η, By this way, the hashed image is converted into dehazed image.

The individual components in the CLGNN-CNN model, including the Graph Convolutional Layer (GCL), Graph Pooling Layer (GPL), and Fully Connected Layer (FCL), collectively enhance feature extraction, cross-layer fusion, and classification, contributing synergistically to improved dehazing performance [35]. The integration of these components enables effective handling of haze by leveraging graph-based information processing, leading to enhanced visibility in hazy scenes.

4. Result and discussion

This section examines image dehazing utilizing a convolutional neural network architecture based on a cross-layer graphical neural network, and compares the performance of the suggested method to that of other systems currently in use. The tests were carried out in Jupyter Notebook on a PC using the specifications listed in Table 1 below.

The existing methods are Defog-SN Algorithm (Defog-SNA), Feedback Spatial Attention Dehazing Network (FSAD-NET), and Generative Adversarial Network Image Dehazing (GANID). The parameters are Accuracy, precision, recall, f1-score, PSNR, and SSIM.

- True positive- TP: The class for which the model's predictions were true is represented by the positive predictions in TP.
- True Negative- TN: The class's negative predictions, which the model correctly identifies, are shown by TP.
- False Positive- FP: FP displays the class's incorrectly classified negative predictions made by the classifier.
- False Negative- FN: The model wrongly identifies the class as negative, but FN shows the positive forecast for it.

Accuracy can be expressed as the proportion of precisely predicted occurrences to all predicted instances. The following formula can be used to compute it:

$$\text{Accuracy} = \frac{\text{TP} + \text{TN}}{\text{TP} + \text{TN} + \text{FP} + \text{FN}} \tag{22}$$

The Analysis of Competency in Recommended and Conventional Methods is shown in Figure 7. The suggested approach CLGNN-CNN has an accuracy

Table 1. Requirements for simulation.

Parameters	Value
RAM	8GB
Memory	200GB
OS	Windows 10 with 64-bit

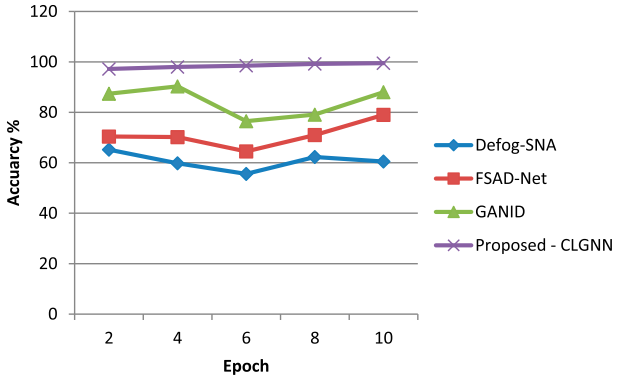

Figure 7. Accuracy in Suggested and Traditional Methods.

Table 2. Evaluation of Proposed CLGNN method using accuracy with other popular methods for dehazing.

Epoch	Defog-SNA	FSAD-Net	GANID	Proposed – CLGNN
2	65.2	70.4	87.4	97.2
4	59.8	70.2	90.3	98
6	55.6	64.5	76.5	98.5
8	62.3	71	79.1	99.2
10	60.5	79	88	99.5

rate of 99.8% when compared to existing approaches like Defog-SNA, FSAD-NET, and GANID, which have accuracy ratings of 60%, 79%, and 89%, respectively. Given this, the recommended method for removing hazing is more effective than revolutionary methods. Table 2 shows the comparative results of accuracy in traditional methods and proposed methods.

The ratio of positive cases to all instances that were predicted to be positive is known as precision. The formula below may be used to compute it:

$$Precision = \frac{TP}{TP + FP} \tag{23}$$

Table 3. Evaluation of the Proposed CLGNN method using Precision with other popular methods for dehazing.

Epoch	Defog-SNA	FSAD-Net	GANID	Proposed – CLGNN
2	65.2	70.4	87.4	97.2
4	59.8	70.2	90.3	98
6	55.6	64.5	76.5	98.5
8	62.3	71	79.1	99.2
10	60.5	79	88	99.5

Figure 8 portrays the Assessment of precision in Suggested and Traditional Methods. When compared to current techniques such as Defog- SNA, FSAD-NET, and GANID, which have precision rates of 62%, 78%, and 90%, respectively, the recommended approach CLGNN-CNN has a rate of 97%. In terms of dehazing the image, the suggested way is more effective than the contemporary methods. Table 3 shows the comparative results of accuracy in traditional methods and proposed methods.

It displays the proportion of occurrences of true positives with accurate labels. It may be computed as:

$$Recall = \frac{TP}{TP + FN} \tag{24}$$

The comparison of recall in suggested and traditional methods is shown in Figure 9. The suggested approach CLGNN-CNN has a rate of 97% recall compared to existing techniques like Defog-SNA, FSAD-NET, and GANID, which have recall values of 63%, 79%, and 91%, respectively. This indicates that the suggested technique works much better for image dehazing than the other method currently in use. The accuracy results of the suggested method and the traditional methods are compared in Table 4.

It combines recall and accuracy, and it is regarded as a model's balanced and accurate performance. The F1

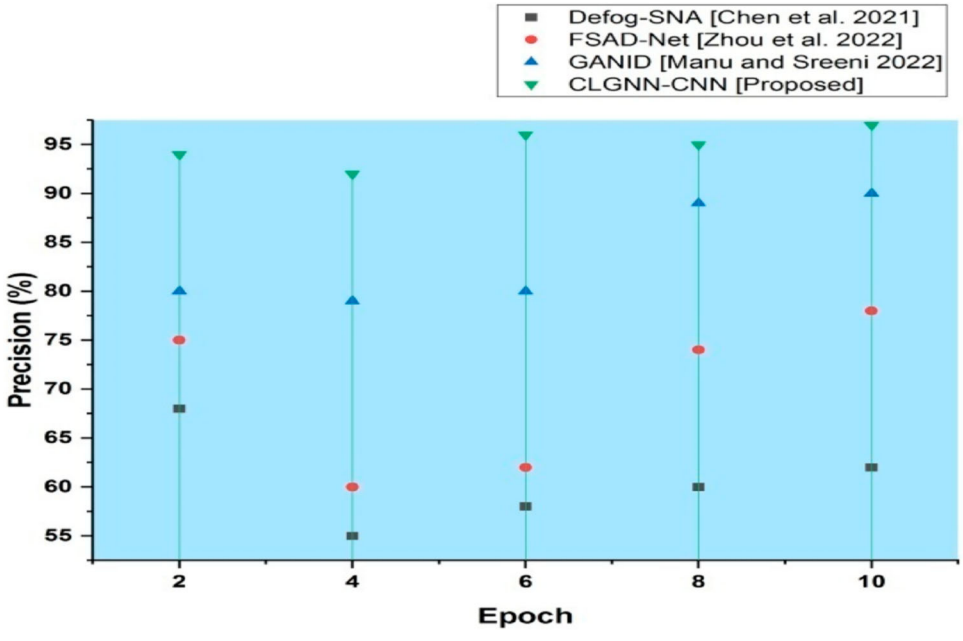

Figure 8. Precision in Suggested and Traditional Methods.

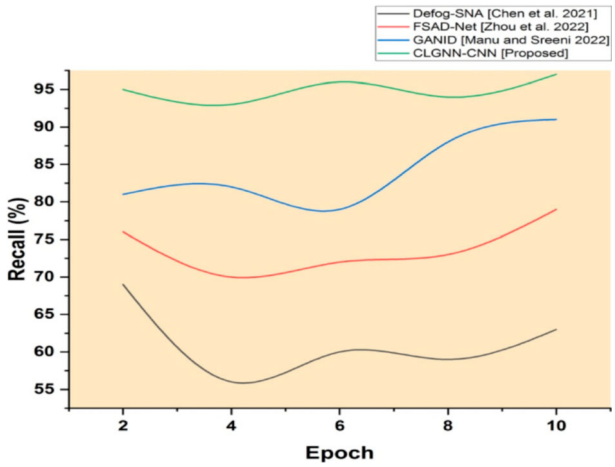

Figure 9. Recall in Suggested and Traditional Methods.

Table 4. Evaluation of Proposed CLGNN method using Recall with other popular methods for dehazing.

Epoch	Defog-SNA	FSAD-Net	GANID	Proposed – CLGNN
2	65.2	70.4	87.4	97.2
4	59.8	70.2	90.3	98
6	55.6	64.5	76.5	98.5
8	62.3	71	79.1	99.2
10	60.5	79	88	99.5

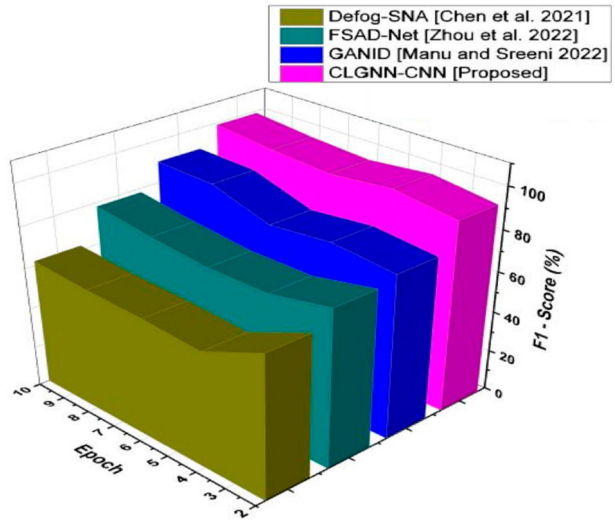

Figure 10. F1-score in Suggested and Traditional Methods.

Table 5. Evaluation of Proposed CLGNN method using F1-Score with other popular methods for dehazing.

Epoch	Defog-SNA	FSAD-Net	GANID	Proposed – CLGNN
2	60.2	72	80	90
4	55.2	75	81	92
6	55	76.5	79	95
8	54	77	85	96
10	62	78	90	99

score is the harmonious average of recall and accuracy. It could be ascertained by using

$$F1score = 2 \times \frac{Precision \times Recall}{Precision + Recall} \tag{25}$$

The disparity of the f1-score in the recommended and standard techniques is shown in Figure 10. The suggested method CLGNN-CNN has a rate of 99 percent when compared to existing techniques like Defog-SNA, FSAD-NET, and GANID, which have 62%, 78%, and 90%, respectively. Thus, the proposed method for image dehazing achieves better performance than the currently available methods. The F1-Score comparison results between the suggested method and the conventional methods are displayed in Table 5.

The PSNR (Peak Signal to Noise Ratio) measures the maximum difference in signal strength (in decibels) among two images. A higher PSNR indicates that the method used to recover clear images performed better.

$$PSNR = 10\log_{10}\frac{I_{max}^2}{MSE} \tag{26}$$

Whsquared and MSE represent, respectively, the maximum possible value in the image and the Mean Squared Error (MSE).

Figure 11 depicts the Comparison of PSNR in Suggested and Traditional Methods. When compared to existing approaches such as Defog- SNA, FSAD-NET, GANID, which have values of 10.22, 15.66, 25.75 dB respectively, and the recommended approach CLGNN-CNN has a rate of 32.72 dB. So, the proposed method for image dehazing achieves higher effectiveness than the existing methods. Table 6 shows the comparative results of PSNR in traditional methods and proposed methods.

The SSIM is a parameter for quantitative assessment of outcomes. SSIM is calculated by dividing the original image by the distorted image, which has been transformed into a vector. Figure 12 depicts the Evaluation of SSIM in Suggested and Traditional Methods. When compared to current techniques such as Defog- SNA, FSAD-NET, and GANID, which have values of 0.4,

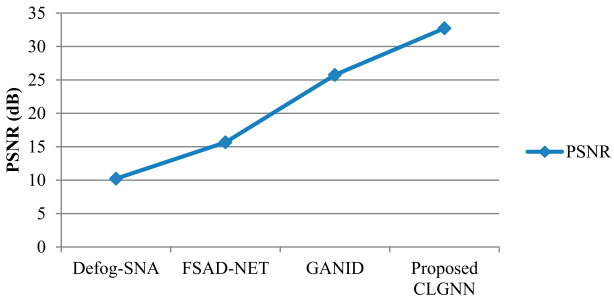

Figure 11. PSNR in Suggested and Traditional Methods.

Table 6. Evaluation of the Proposed CLGNN method using PSNR with other popular methods for dehazing.

Method	PSNR
Defog-SNA	10.22
FSAD-NET	15.66
GANID	25.75
Proposed CLGNN	32.72

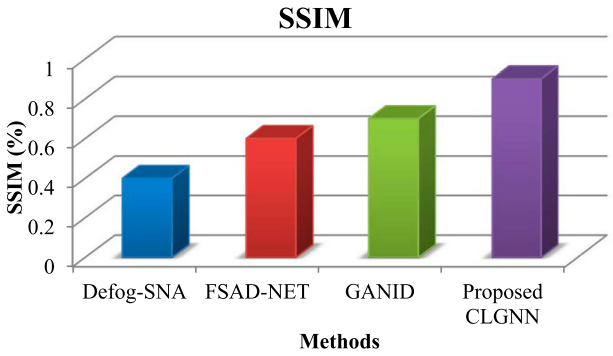

Figure 12. SSIM in Suggested and Traditional Methods.

Table 7. Evaluation of Proposed CLGNN method using PSNR with other popular methods for dehazing.

Method	SSIM
Defog-SNA	0.4
FSAD-NET	0.6
GANID	0.7
Proposed CLGNN	0.9

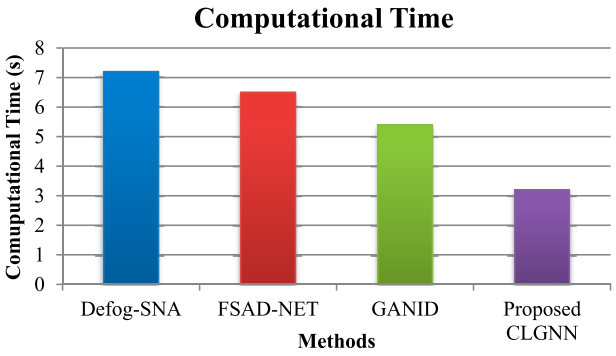

Figure 13. Computational Time in Suggested and Traditional Methods.

0.6, and 0.7 respectively, the recommended approach CLGNN-CNN has a rate of 0.9. As a result, the proposed image dehazing method outperforms the contemporary methods. Table 7 shows the comparative results of PSNR in traditional methods and proposed methods.

The proposed CLGNN-CNN method outperforms existing dehazing techniques, achieving significantly higher accuracy (99.8%) compared to Defog-SNA (60%), FSAD-NET (79%), and GANID (89%). It excels in precision (97%) compared to Defog-SNA (62%), FSAD-NET (78%), and GANID (90%), indicating superior performance in correctly identifying haze-free pixels. The method exhibits notable improvements in recall (97%) compared to Defog-SNA (63%), FSAD-NET (79%), and GANID (91%), emphasizing its effectiveness in retrieving true positive instances Figure 13.

The compared dehazing algorithms differ greatly in terms of computing time. FSAD-NET takes 6.5 s, whereas GANID takes 5.4 s. Defog-SNA takes 7.2 s. By comparison, the CLGNN approach that has been suggested performs noticeably better, taking only 3.2 s to compute. This shows how effective the suggested CLGNN methodology is in dehazing images when compared to other approaches, suggesting advantages for real-time applications and the optimization of CPU resources.

4.1. Ablation study

The purpose of this research's ablation study is to evaluate the efficacy of various additions or changes to the suggested CLGNN-CNN picture dehazing approach. The study assesses the effects of systematically deleting or changing particular model components, such as individual layers, loss functions, or architectural aspects, on performance parameters including computational efficiency, accuracy, precision, and recall. Through a thorough research, it is possible to gain a greater understanding of how each component contributes to the overall success of the CLGNN-CNN technique. This allows for the identification of essential aspects that are necessary to achieve superior outcomes in picture dehazing tasks. The ablation study's results support the design decisions made for the suggested method and can direct future improvements or optimizations aimed at achieving even better dehazing results.

The discriminator's structure is improved using the Defog-SN method. In the end, this results in a more stable model by ensuring that the entire discriminant network satisfies the 1-Lipschitz continuum. Models that were prone to collapse and unstable training were produced by the discriminant network's poor control performance Chen et al. [36]. FSAD allows us to prioritize and selectively process information at a specific location. The core spatial deficiency is caused by the malfunctioning of a dorsal frontal-parietal network, which regulates attention and eye movements as well as depicts stimuli saliency. According to Zhou et al. [37], this deficiency shows up as a bias in spatial attention and salience that is represented in an egocentric coordinate frame. Density Estimation is still unable to accurately forecast the density of the assessed model and claims that this picture is sufficiently dense to continue using. Using the data's statistical distribution as a starting point, generative adversarial networks are implicit probability models that produce data samples. They are used to duplicate variations found in the dataset. When the horizontal vision on the ground level is larger than 1 km, they combine the generator and discriminator networks to increase the visibility that has been harmed by meteorological circumstances Manu and Sreeni [38]. A semi-supervised learning technique called CLGNN-CNN can be used on graph-structured data. Because it is based on an efficient variation of CNN that is used in picture dehazing and is employed in a way that was specially developed to handle pixel data, CLGNN-CNN is superior to other approaches that are currently in use.

5. Conclusion

Haze, on the one hand, is an integral aesthetic aspect that may be utilized to create special effects for specific films, such as those in the science fiction and animation genres. On the other hand, under severe environments, a large quantity of labelled data sets is necessary to advance item detection and identification technologies. A great deal of hazy marked data may be generated by image hazing. The novel image dehazing technique that is presented in this work is based on the CLGNN-CNN. Experimental findings demonstrate that the proposed method reduces the computational time needed to recover the original, haze-free colour image. The primary flaw in the recommended method is that some shadowing is still visible around the edges of the dehazed image. Future research will concentrate on enhancing edge smoothing and detail retention.

Acknowledgement

There is no acknowledgement involved in this work.

Authorship contributions

All authors contributed equally to this work.

Disclosure statement

No potential conflict of interest was reported by the author(s).

Ethics approval and consent to participate

No participation of humans takes place in this implementation process.

Human and animal rights

No violation of Human and Animal Rights is involved.

Data availability statement

Data sharing is not applicable to this article as no datasets were generated or analyzed during the current study.

References

[1] Lien CY, Yang FJ, Huang CC. An efficient image dehazing method. In 2012 Sixth International Conference on Genetic and Evolutionary Computing; IEEE; 2012, August. p. 348–351.

[2] Kponou EA, Wang Z, Wei P. Efficient real-time single-image dehazing based on color cube constraint. In 2017 IEEE 2nd International Conference on Signal and Image Processing (ICSIP); IEEE; 2017, August. p. 106–110.

[3] Xiao J, Zhou J, Lei J, et al. Image hazing algorithm based on generative adversarial networks. IEEE Access. 2019;8:15883–15894. doi:10.1109/ACCESS.2019.2962784

[4] Meng J, Li Y, Liang H, et al. Single-Image dehazing based on two-stream convolutional neural network. J Artif Intel Technol. 2022;2(3):100–110.

[5] Berman D, Treibitz T, Avidan S. Single image dehazing using haze-lines. IEEE Trans Pattern Anal Mach Intell. 2018;42(3):720–734. doi:10.1109/TPAMI.2018.2882478

[6] Zhu Q, Mai J, Shao L. A fast single image haze removal algorithm using color attenuation prior. IEEE Trans Image Process. 2015;24(11):3522–3533. doi:10.1109/TIP.2015.2446191

[7] Cheng S, Yang B. An efficient single image dehazing algorithm based on transmission map estimation with image fusion. Eng Sci Technol Int J. 2022;35:101190.

[8] Huo F, Zhu X, Zeng H, et al. Fast fusion-based dehazing with histogram modification and improved atmospheric illumination prior. IEEE Sensors J. 2020;21(4):5259–5270. doi:10.1109/JSEN.2020.3033713

[9] Zhu Z, Wei H, Hu G, et al. A novel fast single image dehazing algorithm based on artificial multiexposure image fusion. IEEE Trans Instrum Meas. 2020;70:1–23. doi:10.1109/TIM.2020.2991290

[10] Chen J, Yang G, Xia M, et al. HDNet: a dual-stream network with progressive fusion for image hazing detection. J Inform Secur Appl. 2022;69:103271.som.

[11] Soma P, Jatoth RK. An efficient and contrast-enhanced video de-hazing based on transmission estimation using HSL color model. Vis Comput. 2022;38(7):2569–2580. doi:10.1007/s00371-021-02132-3

[12] Singh K, Khare V, Agarwal V, et al. A review on GAN based image dehazing. In 2022 6th International Conference on Intelligent Computing and Control Systems (ICICCS); IEEE; 2022, May. p. 1565–1571.

[13] Preethi B, Anuradha C, Harshitha I, et al. Underwater image enhancement and super resolution based on deep CNN method. In 2022 8th International Conference on Smart Structures and Systems (ICSSS); IEEE; 2022, April. p. 01–04.

[14] Parihar AS, Singh K, Ganotra A, et al. Contrast aware image dehazing using generative adversarial network. In 2022 2nd International Conference on Intelligent Technologies (CONIT); IEEE; 2022, June. p. 1–6.

[15] Gao X, Tang P, Cheng Q, et al. Air infrared small target local dehazing based on multiple-factor fusion cascade network. Neural Comput Appl. 2023;35(12):8657–8665.

[16] Joy AB, Jayasree M. Deep multi-scale residual learning for single image de-hazing. In 2022 International Conference on Computing, Communication, Security and Intelligent Systems (IC3SIS); IEEE; 2022, June. p. 1–6.

[17] Ayoub A, Naeem EA, El-Shafai W, et al. (2022). Video quality enhancement using an optimized dehazing algorithm.

[18] Yoon S, Cho J. Deep multimodal detection in reduced visibility using thermal depth estimation for autonomous driving. Sensors. 2022;22(14):5084. doi:10.3390/s22145084

[19] Guo C, Lian J, Li W. Single image dehazing based on multi-scale channel attention mechanism. In 2022 3rd International Conference on Computer Vision, Image and Deep Learning & International Conference on Computer Engineering and Applications (CVIDL & ICCEA); IEEE; 2022, May. p. 568–573.

[20] Alenezi F, Armghan A, Mohanty SN, et al. Block-greedy and CNN based underwater image dehazing for novel depth estimation and optimal ambient light. Water. 2021;13(23):3470. doi:10.3390/w13233470

[21] Zheng Z, Ren W, Cao X, et al. Ultra-high-definition image dehazing via multi-guided bilateral learning. In 2021 IEEE/CVF Conference on Computer Vision and Pattern Recognition (CVPR); IEEE; 2021, June; p. 16180–16189.
[22] Soma P, Jatoth RK. Implementation of a novel, fast and efficient image de-hazing algorithm on embedded hardware platforms. Circuits Syst Signal Process. 2021;40(3):1278–1294. doi:10.1007/s00034-020-01517-4
[23] Likhitaa PS, Anand R. A comparative analysis of image dehazing using image processing and deep learning techniques. In 2021 6th International Conference on Communication and Electronics Systems (ICCES); IEEE; 2021, July. p. 1611–1616.
[24] Ismail M, Zakir A, Moqa S, et al. Encoder decoder based CNN for single image dehazing with a semi-supervised approach. In 2021 International Conference on Innovative Computing (ICIC); IEEE; 2021, November. p. 1–7.
[25] Zhai X, Rajaram A, Ramesh K. Cognitive model for human behavior analysis. J Interconnect Netw. 2022;22(Supp04):2146013. doi:10.1142/S0219265921460130
[26] Bi G, Wang L, Chen C, et al. Fast single-image dehazing algorithm based on piecewise transformation in optical model. IEEE Photonics J. 2021;13(2):1–19. doi:10.1109/JPHOT.2021.3071384
[27] Li W, Wei H, Qi G, et al. A fast image dehazing algorithm for highway tunnel based on artificial multi-exposure image fusion. In IOP Conference Series: Materials Science and Engineering; IOP Publishing; 2020. Vol. 741, No. 1, p. 012038.
[28] Zheng M, Qi G, Zhu Z, et al. Image dehazing by an artificial image fusion method based on adaptive structure decomposition. IEEE Sensors J. 2020;20(14):8062–8072. doi:10.1109/JSEN.2020.2981719
[29] Zhu Z, Luo Y, Wei H, et al. Atmospheric light estimation based remote sensing image dehazing. Remote Sens (Basel). 2021;13(13):2432. doi:10.3390/rs13132432
[30] Wang W, Yuan X, Wu X, et al. Fast image dehazing method based on linear transformation. IEEE Trans Multimed. 2017;19(6):1142–1155. doi:10.1109/TMM.2017.2652069
[31] Galdran A. Image dehazing by artificial multiple-exposure image fusion. Signal Process. 2018;149:135–147. doi:10.1016/j.sigpro.2018.03.008
[32] Kalaivani K, Kshirsagarr PR, Sirisha Devi J, et al. Prediction of biomedical signals using deep learning techniques. J Intell Fuzzy Syst. 2023;(Preprint):1–14.
[33] Zekrifa DMS, Dhanalakshmi M, Puviarasi R, et al. Optimized controller design for renewable energy systems by using deep reinforcement learning technique. Int J Renew Energ Res (IJRER). 2024;14(1):101–110.
[34] Umaamaheshvari A, Sivasankari K, Suguna N, et al. Optimization technique for optimal location selection based on medical image watermarking on healthcare system. J Intell Fuzzy Syst. 2023;(Preprint):1–11.
[35] Gupta S, Patel N, Kumar A, et al. Adaptive fuzzy convolutional neural network for medical image classification. J Intell Fuzzy Syst. 2023;45(6):1–17.
[36] Chen S, Fan W, Peter S, et al. Defognet: a single-image dehazing algorithm with cyclic structure and cross-layer connections. Complexity. 2021;2021:1–13.
[37] Zhou Y, Chen Z, Li P, et al. FSAD-Net: feedback spatial attention dehazing network. IEEE Trans Neural Netw Learn Syst. 2022.
[38] Manu CM, Sreeni KG. GANID: a novel generative adversarial network for image dehazing. Vis Comput. 2023;39(9):3923–3936.